MODELLING OF NEAR-WALL TURBULENCE WITH LARGE-EDDY VELOCITY MODES

Marta Wacławczyk
Jacek Pozorski

Institute of Fluid Flow Machinery, Polish Academy of Sciences, Gdańsk, Poland
e-mail: mw@imp.gda.pl; jp@imp.gda.pl

In the paper, low-order modelling of the turbulent velocity field in the near-wall region is performed using the Proper Orthogonal Decomposition (POD) approach. First, an empirical eigenfunction basis is computed, basing on two-point velocity correlations. Next, the Galerkin projection of the Navier-Stokes equations on the truncated basis is performed. This results in a system of Ordinary Differential Equations (ODEs) for time-dependent coefficients. Evolution of the largest vortical structures in the near-wall zone is then obtained from the time dependent coefficients and eigenfunctions. The system applied in the present work consists of 20 ODEs, the reconstructed velocity field is two-dimensional in the plane perpendicular to the main flow direction. Moreover, the filtering procedure associated with the POD method is discussed, the POD filter is derived and compared with LES filters.

Key words: proper orthogonal decomposition, coherent structures, turbulent channel flow

1. Introduction

In the near-wall buffer and logarithmic regions, generation of turbulent energy and transport of heat and momentum are mainly controlled by the dynamics of large turbulent eddies. Analysis of experimental data performed by Bakewell and Lumley (1967) proved that these so-called coherent vortices have the characteristic shape of rolls elongated in the streamwise direction. The insight into the instantaneous phenomena in the near-wall zone is useful in many applications, including the study of heat transfer (Kasagi *et al.*, 1988), diffusion and dispersion problems (Joia *et al.*, 1998; Picciotto *et al.*, 2005; Łuniewski *et al.*, 2006) as well as study of flow control (Gunes and Rist, 2004). However, the numerical cost associated with the Direct Numerical Simulations (DNS)

as well as Large Eddy Simulations (LES) of the near-wall region is very high. Hence, there is a need for other simplified methods which would predict, at least qualitatively, the time evolution of the largest eddies.

A development along these lines is the POD approach (Aubry *et al.*, 1988). The method is based on the Lumley (1967) proposal to expand velocity in a series of eigenfunctions computed from the eigenvalue problem with experimentally determined two-point correlations. The problem is defined in such a way that the function basis is optimal for the representation of kinetic turbulent energy for a given flow. Initially, the POD method was used to educt coherent structures from the turbulent field (Bakewell and Lumley, 1967; Moin and Moser, 1989; Deville and Bonnet, 2002). Another application of the POD is to construct a low-order system of ODEs and resolve the dynamics of the largest coherent structures. For this purpose, the momentum equation is subjected to the Galerkin projection on the eigenfunction basis and a set of ordinary differential equations are solved for time-dependent coefficients. The instantaneous velocity field can be then reconstructed from eigenfunctions and their time-dependent coefficients. The POD method was applied to simulations of various flow configurations like, e.g., boundary layers and channel flows (Holmes *et al.*, 1996; Podvin, 2001; Aubry *et al.*, 1988; Ball *et al.*, 1991; Webber *et al.*, 1997), mixing layers and jets (Citriniti and George, 2000; Deville *et al.*, 2000), ventilated cavities (Allery *et al.*, 2006) and other flow cases. The drawback of such simulations is that they can be applied only to a specific geometry for which the two-point statistics have been predetermined experimentally. Yet, this approach can still be very useful, e.g., for analysing dynamics of passive scalars.

The present paper deals with POD simulations of the velocity field in the near-wall region of a turbulent channel flow. It can be regarded as continuation of the previous work (Wacławczyk and Pozorski, 2002) where two-point velocity correlations were computed from the PIV experiment and a typical picture of large eddies was reconstructed; however, simulations of dynamical system were not performed. In this work, the DNS results of the turbulent channel flow at $\mathrm{Re}_\tau = 140$ (courtesy of Dr. Bérengère Podvin) are used to compute the necessary input data for POD: the two-point correlations, eigenfunctions characteristic for the near-wall flow, and coefficients of the ODEs. Contrary to the work of Aubry *et al.* (1988) where the simulations in the near-wall region were performed with 10 POD modes, 20 active modes are employed here. Henceforth, the present approach is called 20D model. The dynamics of large eddies is reconstructed from the time-dependent solution of ODEs and the spatially-dependent eigenfunction basis. The simulations are two-dimensional; this decreases the numerical cost but, on the other hand, the resulting picture of turbulent motion is only qualitative. Another contribution of the present work is the derivation of the filter function associated with the

POD method. This is done in order to discuss the relations between the POD and LES methods.

2. Eigenfunction expansion

The POD is a method of analysis of stochastic fields, which leads to the empirical eigenfunction basis, optimal for the energy representation (Berkooz *et al.*, 1993; Holmes *et al.*, 1996); this means that the series of basis functions converge more rapidly (in the quadratic mean) than any other representation. The POD method relies on numerically or experimentally determined two-point velocity correlations, so the basis is not given analytically (unlike the Fourier basis or the Chebyshev polynomials used in numerical spectral methods for LES and DNS). If we recall that the coherent structures can be defined as high-energy regions, the choice of the POD basis, optimal in the energy representation, seems to be adequate to describe the dynamics of large eddies.

In order to explain in more detail how the two-point correlations are involved into the considerations, we first express the fluctuating velocity of a turbulent field realisation ω as a linear combination of empirical orthogonal functions $\psi^{(n)}(x)$ with random and statistically independent coefficients $a_\omega^{(n)}$

$$u_\omega(x) = \sum_{n=1}^{\infty} a_\omega^{(n)} \psi^{(n)}(x) \tag{2.1}$$

where

$$\left(\psi^{(n)}(x), \psi^{(l)}(x)\right) = \int_\Omega \psi^{(n)}(x)\psi^{(l)*}(x)\, dx = \delta_{nl} \tag{2.2}$$

the parenthesis $(\cdot, \cdot)$ denotes the scalar product; x could either be a position vector or any spatial or temporal coordinate; Ω is the domain of integration, $*$ denotes the complex conjugate and δ_{nl} is the Kronecker delta. To find the optimal basis, we seek for functions $\psi^{(n)}$ which maximise the expression

$$\frac{\langle (u_\omega, \psi^{(n)})(u_\omega, \psi^{(n)})^* \rangle}{(\psi^{(n)}, \psi^{(n)})} = \langle (a_\omega^{(n)})^2 \rangle = \lambda^{(n)} \tag{2.3}$$

(the Einstein sum notation convention does not apply here). Next, the variational method (Lumley, 1970) is used in order to find the maximum of λ; this leads to the eigenfunction and eigenvalue problem with the two-point correlations

$$\left(\langle u(x)u(x')\rangle, \psi^*(x')\right) = \lambda\psi(x) \tag{2.4}$$

The solution to (2.4) gives a class of functions $\psi^{(n)}(x)$ which form, for a given flow case, the optimal POD basis. The basis can be further truncated since only a few first eigenfunctions contain the majority of kinetic energy of the turbulent flow field and characterise its inhomogeneity. In the particular case of homogeneous turbulent fields, Eq. (2.4) is satisfied by the Fourier basis.

The considerations can be readily extended to the case of 3D fully developed turbulent channel flow, statistically homogeneous in the streamwise and spanwise directions. The fluctuating velocity $u_i = U_i - \langle U_i \rangle$ reads

$$u_i(x, y, z, t) =$$
$$= \frac{1}{\sqrt{L_x L_z}} \sum_{n=1}^{\infty} \sum_{k_x=-\infty}^{\infty} \sum_{k_z=-\infty}^{\infty} a_{nk_xk_z}(t) \psi_{ik_xk_z}^{(n)}(y) \exp\left(\mathrm{i}x\frac{2\pi k_x}{L_x} + \mathrm{i}z\frac{2\pi k_z}{L_z}\right) =$$
$$= \frac{1}{\sqrt{L_x L_z}} \sum_p a_p(t) \phi_i^{(p)}(y) \tag{2.5}$$

where L_x and L_z denote the size of the domain (in wall units), in x and z direction respectively, $\sum_p$ stands for the triple sum $\sum_n \sum_{k_x} \sum_{k_z}$, and the symbol $\phi_i^{(p)}(y)$ is introduced for brevity. The intervals $x-x'$ and $z-z'$ denoted by Δx and Δz, respectively, are related to the wavenumbers k_x, k_z by the formulae $\Delta x = L_x/k_x$ and $\Delta z = L_z/k_z$. In the fully developed turbulent channel flow, the eigenvalue problem (2.4) is solved in the y direction only, for each pair of k_x and k_z

$$\int_0^{L_y} \Phi_{ij}(k_x, y, y', k_z)\psi_{jk_xk_z}(y') \, dy' = \lambda\psi_{ik_xk_z}(y) \tag{2.6}$$

where L_y denotes the domain length in the wall-normal direction and Φ_{ij} is the Fourier transform of the two-point velocity correlation tensor Q_{ij}

$$\Phi_{ij}(k_x, y, y', k_z) = \mathcal{F}_{xz}\{Q_{ij}(\Delta x, y, y', \Delta z)\} =$$
$$= \langle \mathcal{F}_{xz}\{u_i(x, y, z)\}\mathcal{F}_{xz}^*\{u_j(x', y', z')\}\rangle$$

The Fourier transform of a given quantity $A(x, z)$ is defined as

$$\mathcal{F}_{xz}\{A(x, z)\} = \frac{1}{\sqrt{L_x L_z}} \int_0^{L_x}\int_0^{L_z} A(x, z) \exp\left(-\mathrm{i}x\frac{2\pi k_x}{L_x} - \mathrm{i}z\frac{2\pi k_z}{L_z}\right) dx \, dz \tag{2.7}$$

The complex coefficients $a_{nk_xk_z}(t)$ in Eq. (2.5) determine the time evolution of the fluctuation field and are themselves governed by a system of ordinary differential equations. These ODEs are obtained by introducing the eigenfunction expansion into the Navier-Stokes equation for fluctuating velocity (Aubry et al., 1988) and subjecting the resulting formula to the Galerkin projection (details are presented in Section 3).

3. Galerkin projection

3.1. Governing equations

As stated in Section 1, the second application of the POD method is the reduced-order modelling. In this case, the time evolution of complex coefficients $a_{nk_xk_z}(t)$ is sought for and the instantaneous velocity field of large eddies is reconstructed from Eq. (2.5). In a general case, the knowledge of the complete two-point correlations $Q_{ij}(x, x', y, y', z, z')$, i.e. a tensor function of 6 variables, is required to fully model the large eddy dynamics. However, in the case of homogeneity in the streamwise and spanwise directions, the tensor Q_{ij} becomes a function of $\Delta x = x - x'$ and $\Delta z = z - z'$. Aubry *et al.* (1988), who considered the turbulent boundary-layer flow, assumed additionally the zero streamwise variation, i.e. analysed only $Q_{ij} = Q_{ij}(0, y, y', \Delta z)$. In spite of this simplification, the resulting velocity field still reveals the major features of near-wall turbulent flow like the intermittent, bursting behaviour.

Now, the derivation of the ordinary differential equations for the coefficients $a_{nk_xk_z}(t)$ will be outlined (cf. Holmes *et al.*, 1996). The new contribution of this theoretical part of the paper is a discussion of relations between the POD and the LES approach. In particular, a formula for the filtering function associated with the POD method is derived. Holmes *et al.* (1996) chose the fully developed turbulent boundary layer as a particular case of study. First, the averaging procedure needs to be defined. As the flow is assumed to be statistically homogeneous in the streamwise and spanwise directions, the mean of a physical quantity $A(x, y, z, t)$ is written as

$$\langle A(y,t) \rangle = \frac{1}{L_xL_z} \int\limits_0^{L_x} \int\limits_0^{L_z} A(x, y, z, t) \; dx \; dz \tag{3.1}$$

and hence it is, in general, a function of time. When the averaged momentum equation is subtracted from the instantaneous one (the Navier-Stokes eq.), we obtain

$$\frac{\partial u_i}{\partial t} + \langle U_1 \rangle \frac{\partial u_i}{\partial x} + \frac{\partial \langle U_1 \rangle}{\partial y} u_2 \delta_{i1} + \left[\frac{\partial u_i u_j}{\partial x_j} - \frac{\partial \langle u_i u_j \rangle}{\partial x_j} \right] = -\frac{1}{\varrho} \frac{\partial p}{\partial x_i} + \nu \frac{\partial^2 u_i}{\partial x_k \partial x_k} \tag{3.2}$$

Here we also assumed that $\langle U_2 \rangle = \langle U_3 \rangle = 0$ and that $\langle U \rangle = \langle U_1 \rangle$ is slowly varying in time, hence its time derivative can be neglected. In the present derivation, following Aubry *et al.* (1988), the mean velocity profile will be described by the analytical formula

$$\langle U \rangle (y) = \frac{1}{\nu} \int\limits_0^y \langle uv \rangle \; dy + \frac{u_*^2}{\nu} \left(y - \frac{y^2}{2H} \right) \tag{3.3}$$

where H is the channel half-width.

The next step is to decompose the fluctuating velocity into the coherent part $u_<$, and the unresolved, background part, $u_>$. The coherent term $u_<$ will be represented by sum (2.5) after truncation at some $n = N$, $k_x = \pm K_x$ and $k_z = \pm K_z$, while the influence of the unresolved scales $u_>$ has to be modelled. In order to derive the evolution equation for $u_<$, Eq. (3.2) will be filtered by analogy to the procedure in LES.

3.2. POD filter

We can assume that the POD method provides a certain kind of filter $G(\boldsymbol{x}, \boldsymbol{x}')$, hence the coherent part of the flow is prescribed as

$$u_{i<}(\boldsymbol{x}) = \int\limits_{\Omega} G_{ij}(\boldsymbol{x}, \boldsymbol{x}') u_j(\boldsymbol{x}') \, d\boldsymbol{x}' \tag{3.4}$$

If we replace $u_<$ by the truncated series of eigenfunctions, the above equation can be rewritten

$$\sum_{k=1}^{N} a_k \phi_{ik}(\boldsymbol{x}) = \sum_{p=1}^{\infty} \int\limits_{\Omega} G_{ij}(\boldsymbol{x}, \boldsymbol{x}') a_p \phi_{jp}(\boldsymbol{x}') \, d\boldsymbol{x}' \tag{3.5}$$

Below, it is proved that the filtering function is given by the formula

$$G_{ij}(\boldsymbol{x}, \boldsymbol{x}') = \sum_{k=1}^{N} \phi_{ik}(\boldsymbol{x}) \phi_{jk}^*(\boldsymbol{x}') \tag{3.6}$$

After substituting (3.6) into (3.5) we obtain

$$\sum_{k=1}^{N} a_k \phi_{ik}(\boldsymbol{x}) = \sum_{p=1}^{\infty} \sum_{k=1}^{N} a_p \phi_{ik}(\boldsymbol{x}) \int\limits_{\Omega} \phi_{jp}(\boldsymbol{x}') \, \phi_{jk}^*(\boldsymbol{x}') \, d\boldsymbol{x}' \tag{3.7}$$

which, from the normalisation condition for eigenfunctions, Eq. (2.2), gives the identity. Hence, we have shown that the POD method provides a particular type of filter (3.6); the result of filtering of a given vector $A_i(\boldsymbol{x}, t)$ will be denoted by $\widetilde{A_i}(\boldsymbol{x}, t)$. In the case of turbulent channel flow, homogeneous in the streamwise and spanwise directions, because of the relation between ψ and ϕ, Eq. (2.5), the filter G_{ij} is given by the formula

$$G_{ij}(\Delta x, y, y', \Delta z) = \tag{3.8}$$

$$= \frac{1}{L_x L_z} \sum_{n=1}^{N} \sum_{k_x=-K_x}^{K_x} \sum_{k_z=-K_z}^{K_z} \psi_{ik_x k_z}^{(n)}(y) \psi_{jk_x k_z}^{(n)}(y') \exp\left(\mathrm{i}\Delta x \frac{2\pi k_x}{L_x} + \mathrm{i}\Delta z \frac{2\pi k_z}{L_z} \right)$$

In this case, G_{ij} is a tensor function of 4 variables; this form might be confusing and not easy to interpret at first sight if we refer to standard homogeneous filters used in LES methods (Pope, 2000). Hence, we have found it instructive to compare the POD expansion with the truncated series expansion of velocity in the Chebyshev space in the y direction and the Fourier space in the x and z directions. Such an expansion is used in spectral DNS and LES methods (Peyret, 2002). As an example, for a non-homogeneous turbulent channel flow with non-moving walls at $y = H$ and $y = -H$ the truncated velocity is expressed as a sum

$$
\widetilde{u}_i(x, y, z) =
$$

$$
= \frac{1}{\sqrt{L_x L_z}} \sum_{n=1}^{N} \sum_{k_x=-K_x}^{K_x} \sum_{k_z=-K_z}^{K_z} a^T_{ink_xk_z}(t) f_n(y) \exp\left(\mathrm{i}x\frac{2\pi k_x}{L_x} + \mathrm{i}z\frac{2\pi k_z}{L_z}\right)
$$

(3.9)

where in the above, the time-dependent coefficients $a^T_{ink_xk_z}(t)$ are vectors $(i = 1, 2, 3)$, while $f_n(y)$ are functions constructed from the Chebyshev polynomials of order $2n$, shifted in a way which assures that velocity at the wall is zero, i.e., $f_n(y) = T_{2n}(y/H) - 1$. The function f_n is the same for all components of velocity and all k_x, k_z. On the contrary, in POD series, cf. Eq. (2.5), $a_{nk_xk_z}(t)$ is a scalar, identical for all components of velocity, while the POD eigenfunctions $\psi^{(n)}_{ik_xk_z}(y)$ are vectors. The eigenvalue problem is solved for each k_x, k_z pair separately which assures that the basis optimally represents the energy contained in each mode and in each component of velocity. Consequently, the filter function in the POD method is a tensor, while the filter function for the truncated Chebyshev-Fourier expansion reads

$$
G(\Delta x, y, y', \Delta z) =
$$

$$
= \frac{1}{\sqrt{L_x L_z}} \sum_{n=1}^{N} \sum_{k_x=-K_x}^{K_x} \sum_{k_z=-K_z}^{K_z} f_n(y) f_n(y') \exp\left(\mathrm{i}\Delta x\frac{2\pi k_x}{L_x} + \mathrm{i}\Delta z\frac{2\pi k_z}{L_z}\right)
$$

(3.10)

In Section 4, we present selected cross-sections of the POD filter based on the computed POD modes and compare it with the filter constructed from the Chebyshev polynomials.

3.3. Filtered equations

When the POD filtering procedure is applied to Eq. (3.2), we obtain the governing equation for the resolved part of the fluctuating velocity field in the near-wall region

$$\frac{\partial \widetilde{u}_i}{\partial t} + \langle U_1 \rangle \frac{\partial \widetilde{u}_i}{\partial x} + \frac{\partial \langle U_1 \rangle}{\partial y} \widetilde{u}_2 \delta_{i1} + \frac{\partial \widetilde{u}_i \widetilde{u}_j}{\partial x_j} - \frac{\partial \langle \widetilde{u}_i \widetilde{u}_j \rangle}{\partial x_j} =$$

$$= \Big[\frac{\partial \widetilde{\widetilde{u}_i \widetilde{u}_j}}{\partial x_j} - \frac{\partial \langle \widetilde{\widetilde{u}_i \widetilde{u}_j} \rangle}{\partial x_j} - \frac{\partial \widetilde{u}_i \widetilde{u}_j}{\partial x_j} + \frac{\partial \langle \widetilde{u}_i \widetilde{u}_j \rangle}{\partial x_j} \Big] - \frac{1}{\varrho} \frac{\partial \widetilde{p}}{\partial x_i} + \nu \frac{\partial^2 \widetilde{u}_i}{\partial x_k \partial x_k} \tag{3.11}$$

The bracketed term on the RHS will be replaced here by a model (cf. Holmes *et al.*, 1996), analogously to the subgrid viscosity closure used in LES (cf. Pope, 2000)

$$[\cdot] = -2\alpha_1 \nu_T \frac{\partial \widetilde{s}_{ij}}{\partial x_j} + \frac{4}{3} \alpha_2 (l_>)^2 \frac{\partial}{\partial x_i} [\widetilde{s}_{kl} \widetilde{s}_{kl} - \langle \widetilde{s}_{kl} \widetilde{s}_{kl} \rangle] = -\alpha_1 \nu_T \frac{\partial^2 \widetilde{u}_i}{\partial x_j \partial x_j} + \frac{\partial p_T}{\partial x_i} \tag{3.12}$$

where $\widetilde{s}_{ij}$ is the resolved strain rate tensor: $\widetilde{s}_{ij} = (\widetilde{u}_{i,j} + \widetilde{u}_{j,i})/2$, α_1 and α_2 are model constants, and $l_>$ is the length scale characteristic of the unresolved motion. The second term on the RHS of Eq. (3.12) involves p_T which is called the pseudo-pressure; the term can be added to the pressure and the two form together the modified kinematic pressure $\mathcal{P} = \widetilde{p}/\varrho + p_T$.

In the POD approach, the subgrid viscosity ν_T is modelled in terms of the first neglected mode

$$\nu_T = u_> l_> = \int_0^{L_y} \langle u_{k>} u_{k>} \rangle \, dy \cdot \sqrt{L_y \int_0^{L_y} \Big\langle \frac{\partial u_{i<}}{\partial x_j} \frac{\partial u_{i<}}{\partial x_j} \Big\rangle \, dy} \tag{3.13}$$

where $u_>$ is the velocity scale of unresolved motion reconstructed from the first neglected mode, and $l_>$ is the length scale of that mode. A justification for such a choice is presented in Holmes *et al.* (1996). Filtered equation (3.2), including the model (3.12) and formula for the mean velocity (3.3) now reads

$$\frac{\partial \widetilde{u}_i}{\partial t} = -\Big[\frac{1}{\nu} \int_0^y \langle \widetilde{u}_1 \widetilde{u}_2 \rangle \, dy + \frac{u_*^2}{\nu} \Big(y - \frac{y^2}{2H} \Big) \Big] \frac{\partial \widetilde{u}_i}{\partial x} +$$

$$- \widetilde{u}_2 \delta_{i1} \Big[\frac{1}{\nu} \langle \widetilde{u}_1 \widetilde{u}_2 \rangle + \frac{u_*^2}{\nu} \Big(1 - \frac{y}{H} \Big) \Big] + \tag{3.14}$$

$$+ (\nu + \alpha_1 \nu_T) \frac{\partial^2 \widetilde{u}_i}{\partial x_k \partial x_k} - \Big[\frac{\partial \widetilde{u}_i \widetilde{u}_j}{\partial x_j} - \frac{\partial \langle \widetilde{u}_i \widetilde{u}_j \rangle}{\partial x_j} \Big] - \frac{\partial \mathcal{P}}{\partial x_i}$$

The coherent part of fluctuations can be replaced by truncated series (2.5)

$$u_{i<}(x, y, z) = \widetilde{u}_i(x, y, z) =$$

$$= \frac{1}{\sqrt{L_x L_z}} \sum_{n=1}^{N} \sum_{k_x=-K_x}^{K_x} \sum_{k_z=-K_z}^{K_z} a_{n k_x k_z}(t) \psi_{i k_x k_z}^{(n)}(y) \exp\Big(i x \frac{2\pi k_x}{L_x} + i z \frac{2\pi k_z}{L_z} \Big) \tag{3.15}$$

From now on, the notation $\widetilde{(\cdot)}$ is skipped for the sake of brevity.

In order to derive the system of ordinary differential equations for the coefficients $a_{nk_xk_z}(t)$, the Fourier transform is applied to Eq. (3.14). This is followed by the Galerkin projection procedure, i.e. the equation is multiplied by the eigenfunction $\psi_{ik_xk_z}^{(m)}(y)$ and integrated over y keeping in mind normalisation condition (2.2). It is noted that in (2.2) the summation over index i is performed, hence, the resulting ODEs do not depend on i. This procedure leads to the set of ordinary differential equations for the coefficients $a_{nk_xk_z}$ (Holmes et $al.$, 1996)

$$
\begin{aligned}
\frac{da_{nk_xk_z}}{dt} &= A_1^{(mn)}(k_x, k_z)a_{mk_xk_z} + (\nu + \alpha_1\nu_T)A_2^{(mn)}(k_x, k_z)a_{mk_xk_z} + \\
&+ B_{k_x'k_z'}^{(lmqn)}(k_x, k_z)a_{lk_xk_z}a_{mk_x'k_z'}a_{qk_x'k_z'}^* + C(t) + \\
&+ D_{k_x'k_z'}^{(lmn)}(k_x, k_z)a_{lk_x'k_z'}a_{m(k_x-k_x')(k_z-k_z')}
\end{aligned}
\tag{3.16}
$$

The coefficients $A_1^{(mn)}$ and $B_{k_x'k_z'}^{(lmqn)}$ represent the effect of the mean velocity profile on eigenmodes, $(\nu + \alpha_1\nu_T)A_2^{(mn)}$ account for the dissipation of kinetic energy. The influence of the unresolved scales on the system is modelled via ν_T; moreover, $D_{k_x'k_z'}^{(lmn)}$, and $B_{k_x'k_z'}^{(lmqn)}$ represent interactions between the basis functions. Finally, the term $C(t)$ represents communication between the inner and the outer region via pressure interactions which can be modelled as impulsive random perturbations (Holmes et $al.$, 1996). By solving the set of equations (3.16), one obtains time evolution of the coefficients $a_{nk_xk_z}$.

4. POD eigenfunctions

Two-point correlations, needed for the POD method are computed from DNS data at $\mathrm{Re}_\tau = 140$ (Podvin, $priv.$ $comm.$). The data contain the Fourier coefficients $\widehat{u}_i(k_x, y, k_z)$ of 200 independent snapshots of the fluctuating velocity field. The velocity was Fourier-transformed in the streamwise and spanwise directions where the flow is assumed to be periodic. The first wavenumbers, $k_x = 1$, $k_z = 1$ correspond to separations $L_x = 600$ in the streamwise and $L_z = 300$ in the spanwise direction. The data file includes spanwise wavenumbers k_z ranging from -5 to 5 and streamwise numbers $k_x = 0, 1, 2$. There are 20 computational points in the wall-normal direction, up to $y^+ = 50$. The current truncation of available coefficients to $K_z = 5$ and $K_x = 2$ is quite drastic, therefore only the velocity field of the largest modes can be computed. Nevertheless, the data are sufficient for the simple POD simulations, with a

limited number of modes, like the 10D or 32D models of Aubry *et al.* (1988), Shangi and Aubry (1993).

The Fourier transform of the two-point correlation tensor is computed as an ensemble average over $N = 200$ realisations

$$\Phi_{ij}(k_x, y, y', k_z) = \frac{1}{N} \sum_{n=1}^{N} \widehat{u}_i^{(n)}(k_x, y, k_z)\widehat{u}_j^{(n)*}(k_x, y', k_z) \qquad (4.1)$$

Additionally, the number of data can be increased by the use of symmetries (cf. Omurtag and Sirovich, 1999). As an example, it follows from the spanwise reflection symmetry that if the functions $u_1(x, y, z)$, $u_2(x, y, z)$, $u_3(x, y, z)$ satisfy the Navier-Stokes equation, then $u_1(x, y, -z)$, $u_2(x, y, -z)$, $-u_3(x, y, -z)$ are also a solution to this equation. The spanwise reflection symmetry results in the following relation for the two-point correlation tensor

$$\Phi_{ij}(k_x, y, y', k_z) = \omega_{ij}\Phi_{ij}(k_x, y, y', -k_z) \qquad (4.2)$$

where $\omega_{ij} = 1$ if i and j are both equal to 3 or both different from 3, otherwise $\omega_{ij} = -1$. Important for further simulations is the property of the two-point correlation tensor in the case of zero streamwise separations ($k_x = 0$). As the velocity field is real, its Fourier transform must satisfy the relation $\widehat{u}_i(k_x, y, k_z) = \widehat{u}_i^*(-k_x, y, -k_z)$ which, together with symmetry (4.2) written for $k_x = 0$, imply that components of the eigenfunction vector $\psi_{1,0,k_z}$ and $\psi_{2,0,k_z}$ are purely real and $\psi_{3,0,k_z}$ is purely imaginary.

Given the statistics $\Phi_{ij}(k_x, y, y', k_z)$, eigenvalue problem (2.6) can be solved for each pair of k_x and k_z. However, as current simulations are restricted to 2D, it is sufficient to compute the eigenvalues and eigenvectors of $\Phi_{ij}(0, y, y', k_z)$ for $k_z = 1, \ldots, 5$. In practice, only the two components $\psi_{1,0k_z}^{(n)}$ and $\psi_{3,0k_z}^{(n)}$ are found from eigenvalue problem (2.6), whereas the second component $\psi_{2,0k_z}^{(n)}$ is computed from the continuity equation (cf. Aubry *et al.*, 1988)

$$2\pi \mathrm{i} k_z \psi_{3,0k_z}^{(n)} + \frac{d\psi_{2,0k_z}^{(n)}}{dy} = 0 \qquad (4.3)$$

For this purpose, for each k_z the above formula is integrated over y.

In each eigenvalue problem (for $k_z = 1, \ldots, 5$), the first two eigenfunctions and eigenvectors (i.e. for the indices $n = 1$ and 2) are computed. Here, the work differs from the approaches of Aubry *et al.* (1988) and Podvin (2001), which were restricted to the first eigenfunction. In the approach of Aubry *et al.*, 10 ordinary differential equations are solved for the real and imaginary parts of the coefficients a_{1k_z}, $k_z = 1, \ldots, 5$. Hence, the model is called 10D. In the current approach the simulations of 20D model are performed and twenty

equations for the real and imaginary parts of a_{1k_z} and a_{2k_z}, $k_z = 1, \ldots, 5$ are solved. As will be shown further, the second eigenfunction $(n = 2)$ improves the reconstructed velocity statistics of the wall-normal and spanwise component. The resulting eigenfunctions are presented in Fig. 1. Their corresponding eigenvalues (which are the energy of modes) are presented in Table 1 as a fraction of the total kinetic energy of the fluctuating field. As could be expected, the eigenfunction for $n = 1$ and $k_z = 2$ is the most energetic one. The same observation was made by Aubry et $al.$ (1988) and Podvin (2001). For $n = 2$ we find that the mode $k_z = 1$ is the most energetic. It is also seen in Table 1 that the eigenmodes $n = 2$ are one order of magnitude smaller than those for $n = 1$.
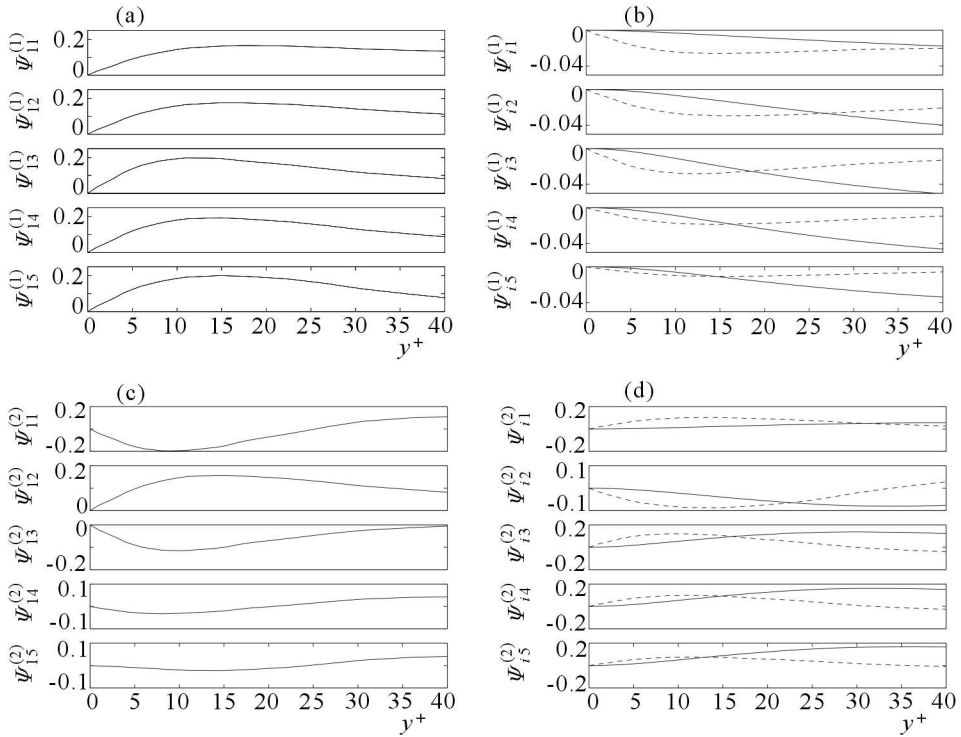
Fig. 1. Eigenfunctions for $k_x = 0$, five different spanwise wavenumbers (from top to bottom) $k_z = 1, \ldots, 5$, $n = 1$; (a) $\Re[\psi_{1,k_z}^{(1)}]$, (b) $\Re[\psi_{2,k_z}^{(1)}]$: (——), $\Im[\psi_{3,k_z}^{(1)}]$: (– – –), and $n = 2$; (c) $\Re[\psi_{1,k_z}^{(2)}]$, (d) $\Re[\psi_{2,k_z}^{(2)}]$: (——), $\Im[\psi_{3,k_z}^{(2)}]$: (– – –)

The filter $G_{ij}(0, y, y', \Delta z)$, cf. Eq. (3.8), can now be reconstructed from the computed eigenfunctions. The cross-sections of the trace $G_{ii}(0, y, y', \Delta z) = G_{ii}(y, y', \Delta z)$ for different values of $y = y'$ are presented in Fig. 2a.

Table 1. The energy of selected modes as a fraction of the total kinetic energy of the fluctuating field

k_z	1	2	3	4	5
$n = 1$	7.99%	15.07%	7.38%	0.74%	0.94%
$n = 2$	1.27%	0.35%	0.22%	0.1%	0.05%

In the z direction, the eigenfunction basis becomes the Fourier basis and the POD method simply provides a sharp spectral cut-off filter. Next, the separation Δz was set to 0 and the trace of the filter $G_{ii}(y, y_0, 0)$ was plotted for a few selected values of y_0, see Fig. 2b. The functions attain zero at $y = 0$. To better illustrate the shape of the function $G_{ii}(y, y', 0)$ its isolines are plotted in Fig. 3. There exists a similarity between this function and the filter constructed from the Chebyshev polynomials, cf. Eq. (3.10). The isolines of such a filter, with the truncation at $N = 6$ are presented in Fig. 4. In order to simplify the comparison with the POD filter, the variable of the Chebyshev polynomials has been appropriately shifted, so that the wall is now placed at $y = 0$. Hence, we have shown that although the form of the POD filter function, Eq. (3.8), may seem complicated at the first sight, it is in fact not far from the filter that follows from the truncated Fourier-Chebyshev expansion of velocity.
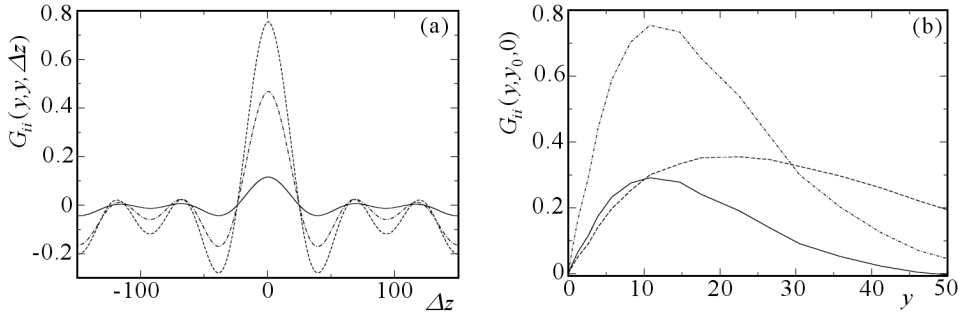
Fig. 2. Cross-sections of the trace $G_{ii}(y, y, \Delta z)$ for (a) $y^+ = 2.6$: (——), 5.7: $(- - \cdot - - \cdot --)$, 10.7: $(- - -)$, (b) cross-sections of the trace $G_{ii}(y, y_0, 0)$ for $y_0^+ = 2.6$: (——), 10.7: $(- - \cdot - - \cdot --)$, 30.5: $(- - -)$

From the eigenfunctions and eigenvectors, the velocity statistics can also be reconstructed. As only a few eigenmodes are used, the reconstructed velocity field contains less energy than the DNS field. The statistics of velocity components are computed from the formula

$$\langle u_i u_j \rangle = \sum_{n=1}^{N} \sum_{k_z=1}^{5} \lambda_{nk_z} \psi_{i,k_z}^{(n)} \psi_{j,k_z}^{(n)*} \tag{4.4}$$

$G_{ii}(y,y',0)$

—	0.7
----	0.6
----	0.5
-----	0.4
-----	0.3
---	0.2
—	0.1
=	0
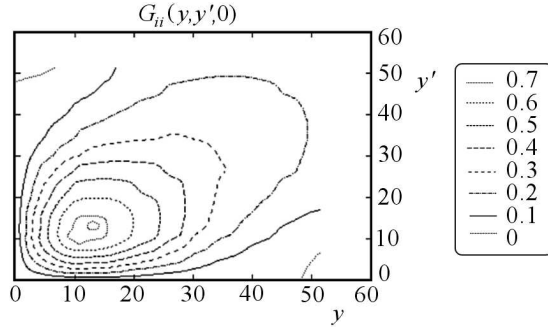
Fig. 3. Isolines of the trace $G_{ii}(y, y', 0)$

$G(y,y',0)$

------	12
....	11
------	10
--·--	9
-·-·-	8
....	7
------	6
....	5
—	4
-----	3
....	2
....	1
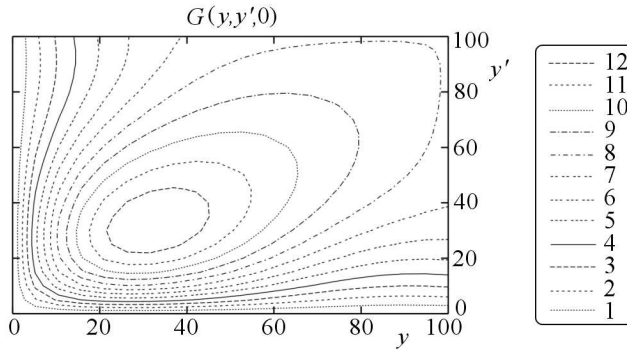
Fig. 4. Isolines of a filter $G(y, y', 0)$ constructed from the shifted Chebyshev polynomials

where $i = 1, 2, 3$ and N is the number of eigenmodes used in the summation ($N = 1$ or $N = 2$). Figure 5a presents the r.m.s. of fluctuating velocity for the streamwise component and the Reynolds-stress component $\langle uv \rangle$, the r.m.s. of wall-normal and spanwise components are presented in Fig. 5b. The statistics reconstructed for $N = 1$ and $N = 2$ are compared with the DNS data of Iwamoto (2002). It is seen that the second eigenmode $n = 2$ improves the wall-normal and spanwise statistics, while the r.m.s. of streamwise component remains almost unchanged. The profiles presented in Fig. 5a compare reasonably with the DNS data. In the region very close to the wall ($y/H < 0.1$ or $y^+ < 15$), the comparison of wall-normal and spanwise fluctuation variance with DNS, cf. Fig. 5b, is also acceptable, if one takes into account the simplicity of the model used in the present study. In the wall vicinity, the flow is dominated by large eddies which form streamwise rolls. Further from the wall, the range of length scales of eddies increases. Hence, the POD method with a few eigenmodes is not able to accurately reproduce the turbulence statistics further away from the wall.
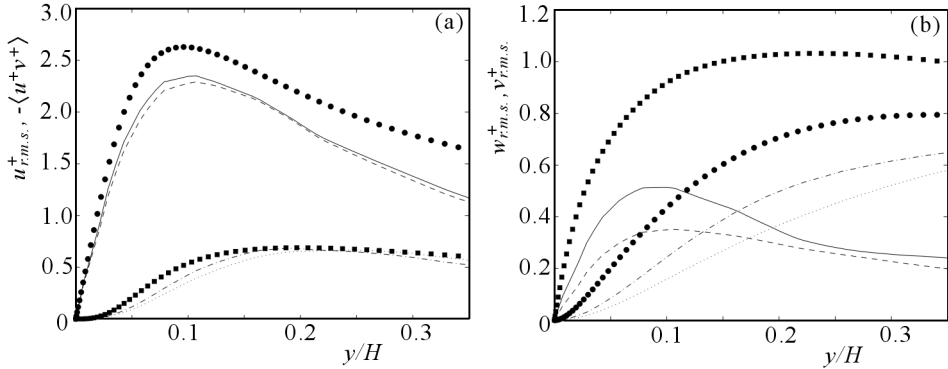
Fig. 5. Turbulent channel flow at $\mathrm{Re}_\tau = 140$. Velocity statistics reconstructed from the POD eigenfunctions with $n = 1$: $(- - -)$ and $n = 2$: (———), compared with the DNS data of Iwamoto (2002): (a) $u^+_{r.m.s.}$: $\bullet$, $-\langle u^+ v^+ \rangle$: $\blacksquare$, (b) $v^+_{r.m.s.}$: $\bullet$, $w^+_{r.m.s.}$: $\blacksquare$

5.   Results of POD simulation

The Navier-Stokes equations can now be projected on the eigenfunction basis which results in a set of ordinary differential equations for the time coefficients a_{nk_z} of the 20D model ($n = 1, 2$; $k_z = 1, \ldots, 5$). As the evaluation of coefficients requires knowledge of the first and second derivatives of eigenfunctions, the computed profiles of $\Psi^{(n)}_{ik_z}(y)$ must be curve-fitted, especially in the near-wall region. For this purpose, the least-squares algorithm is used. The streamwise and spanwise components $\Psi^{(n)}_{ik_z}(y)$ ($i = 1$ or 3) are fitted to curves $a_i y + b_i y^2 + c_i y^3 + d_i y^4$ and the wall-normal component $\Psi^{(n)}_{2k_z}(y)$ is fit to a curve $b_2 y^2 + c_2 y^3 + d_2 y^4$, so that the near-wall scalings $u, w \sim y$ and $v \sim y^2$ are satisfied. We have found in the numerical tests that 4th-order polynomials are a good compromise in the interpolation process.

The next step is to estimate the influence of the unresolved modes by computing the subgrid viscosity. Here, the approach of Holmes $et\ al.$ (1996) is followed and ν_T is estimated from the statistics of the first unresolved mode, cf. Eq. (3.13). The resulting value of ν_T equals approximately 8.6.

The solution to the set of ODEs differs with the varying parameter α. For large values of α ($\alpha > 10$), the coefficients attain constant non-zero values. In the language of the dynamical system theory, this kind of solution is called stable fixed point. As noticed by Aubry $et\ al.$ (1988), in such a case the reconstructed velocity field forms two steady counter-rotating rolls, similar to those obtained in the pioneering work of Bakewell and Lumley (1969). The time evolution of the real parts of selected coefficients for $\alpha = 15$ is presented in Fig. 6a, where $X_{nk_z} = \Re[a_{nk_z}]$.
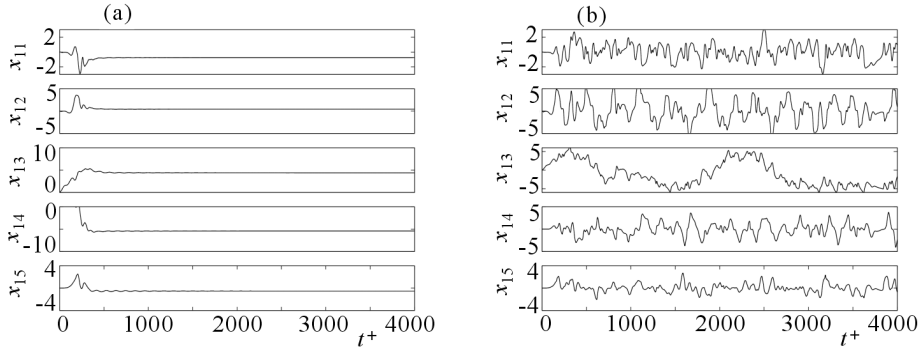
Fig. 6. Selected coefficients a_{nk_z} computed from the set of ODEs in the 20D model for (a) $\alpha = 15$, (b) $\alpha = 0.15$

If we compare dynamical behaviour of the 10D model of Aubry *et al.* (1988) with the current 20D model we find that the former is less noisy. For example, the intermittent region or steady periodic motion (for details see Aubry *et al.*, 1988) was not found in the present approach. Instead, all coefficients for values of α between 0 and 10 fall in a more complex, chaotic region. The more chaotic time behaviour of the coefficients was also observed in the three-dimensional model of 32 modes, which was considered in the paper of Sanghi and Aubry (1993). Figure 6b presents the time behaviour of selected POD coefficients for $\alpha = 0.15$.

A doubt follows from the fact that the solution is in fact sensitive to small changes in values of the coefficients. The point is that in order to compute the coefficients, in particular $A_2^{mn}(k_x, k_z)$, it is necessary to differentiate twice the eigenfunctions. It is recalled that the two-point correlations are computed from a finite number of snapshots, then the eigenvalue problem is solved, the eigenvectors are curve-fitted, the second component $\psi_{2,k_z}^{(n)}$ is computed from the continuity equation, then the first and second order derivatives of eigenfunctions are evaluated. The whole procedure introduces a numerical error. So far, the parameter α was chosen to be $\alpha = 1.5$. The resulting time behaviour of the coefficients is presented in Fig. 7. The real X_{nk_z} and imaginary parts Y_{nk_z} of the coefficients are rescaled, so that $|a_{nk_z}| = X_{nk_z}^2 + Y_{nk_z}^2 = 1$. For the chosen $\alpha = 1.5$, we obtain the lowest value of the time scale associated with the most energetic mode ($k_z = 2$, $n = 1$), equal approximately 250 viscous units. A lower value of the time scale is associated with the mode ($k_z = 1$, $n = 1$) and even lower with the modes $k_z = 4$ and $k_z = 5$. The decrease of the time scale with the increasing wavenumber k_z is also observed in the analysis of coefficients obtained from the direct projection of the DNS velocity field onto the POD modes (cf. Podvin, 2001). In the present dynamical system, the only exception is the third mode which has the largest characteristic time

scale, equal 1300 approximately. Results for modes $k_z = 1, 2, 4$ and 5 are comparable with the experimental data (cf. discussion in the paper of Kasagi *et al.* (1989) which show a scatter of interburst durations in the range 50-150 (in viscous units).
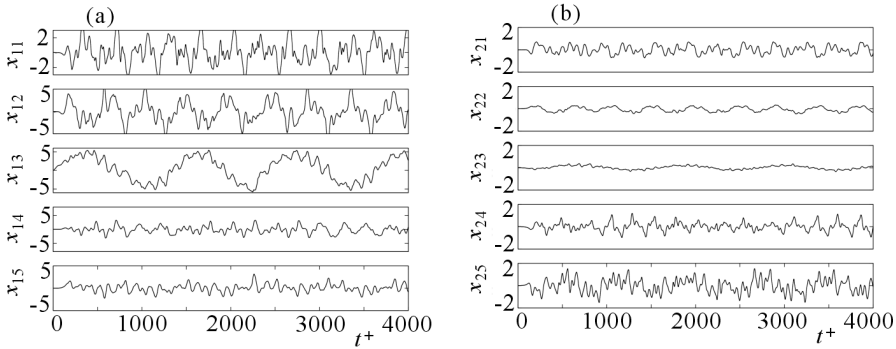
Fig. 7. Real parts of coefficients a_{1k_z} computed from the set of ODEs in the 20D model for $\alpha = 1.5$

The spatial information contained in the POD eigenfunctions together with the time behaviour of POD coefficients obtained from the solution of low-order dynamical system, give a fluctuating velocity field in the near-wall zone, cf. Eq. (3.15). The field reconstructed at a given instant t_0 is presented in Fig. 8. In the current two-dimensional model, only modes with no streamwise dependence ($k_x = 0$) are retained. These modes are associated with the streaks elongated in the streamwise direction that are observed in the wall turbulence (Omurtag and Sirovich, 1999). In the cross-section of the flow, those structures form pairs of counter-rotating rolls which can also be identified in Fig. 8. Their characteristic spanwise length scale is around 100 viscous units, which has also been observed in other POD studies (e.g., Aubry *et al.*, 1988).
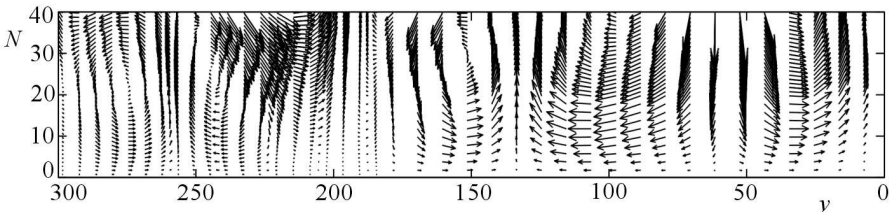
Fig. 8. The reconstructed velocity field for a given instant t_0, cf. Eq. (3.15)

6.   Conclusions and perspectives

In the paper, the POD approach was used to perform simulations of large-eddy dynamics in the near-wall region of a turbulent channel flow. The first step was to compute a two-point velocity correlation tensor from 200 independent snapshots of DNS data. Next, the eigenvalue and eigenfunction problem was solved to obtain an empirical basis that optimally represents kinetic energy in the considered flow domain. The contribution of the present work is also the derivation and discussion concerning the form of the filter function associated with the POD method. The POD filter constructed from the eigenfunctions is generally a tensor. Additionally, each of its components is a function of 8 variables; however, in the case of homogeneity the number of variables is reduced. The form of the filter might be difficult to analyse at first sight, if one compares it with the standard filters used in the LES method on uniform grids. However, as it was shown, the shape of the trace G_{ii} is similar to the filter function associated with the Fourier-Chebyshev expansion of velocity which is used in spectral methods (Peyret, 2001). The tensor form of the POD filter follows from the fact that POD eigenfunctions are vectors, while in the Chebyshev expansion the same basis is used for each component of velocity.

The POD simulations are based on the experimental data of two-point correlations, however some new information about the velocity field can be extracted, like, e.g., the time evolution of large eddies. To study the flow dynamics, the Navier-Stokes equations were projected on the empirical basis to form a set of ordinary differential equations for time-dependent coefficients. Contrary to the work of Aubry *et al.* (1988) who considered the basis of 5 eigenmodes in the z direction and only one eigenmode in the y direction, in the present paper one additional mode in the y direction was considered. Hence, the total number of ODEs solved for real and imaginary parts of the time-dependent POD coefficients was 20. The inclusion of additional modes resulted in a randomisation of time behaviour of coefficients in comparison to the 10D model of Aubry *et al.* (1988). The flow-field resulting from the simulations was two-dimensional, in the plane perpendicular to the main flow direction (y-z plane). This is a result of assumption that the quantities describing the flow are slowly-varying in the x direction in comparison to the variations in the y and z directions. The additional mode improves wall-normal and spanwise components of reconstructed velocity, which is particularly important for further applications like studies on the passive contaminant: in the y-z plane the passive contaminant is traced in the velocity field of those two components (Wacławczyk and Pozorski, 2004).

Analysis of turbulent flows with a passive scalar and two-phase dispersed flows in the near-wall geometry are promising directions for future investiga-

tions. The low numerical cost of a dynamical system based on POD modes allows, e.g. for a detailed study of the passive contaminant field at varying Schmidt/Prandtl numbers. In the case of two-phase flows, a perspective for a future work is examination of preferential particle concentration and their separation at walls.

References

1. ALLERY C., BÉGHEIN C., HAMDOUNI A., VERDON N., 2006, Particle dispersion in turbulent flows by POD low order model using LES snapshots, In: *Direct and Large-Eddy Simulation VI*, E. Lamballais, R. Friedrich, B.J. Geurts and O. Mtais (Edit.), 755-762, Springer, the Netherlands

2. AUBRY N., HOLMES P., LUMLEY J.L., STONE E., 1988, The dynamics of coherent structures in the wall region of turbulent boundary layer, *J. Fluid Mech.*, **192**, 115-173

3. BAKEWELL H.P., LUMLEY J.L., 1967, Viscous sublayer and adjacent wall region in turbulent pipe flow, *Phys. Fluids*, **10**, 1880-1889

4. BALL K., SIROVICH L., KEEFE L., 1991, Dynamical eigenfunction decomposition of turbulent channel flow, *Int. J. Num. Meth. Phys.*, **12**, 585-604

5. BERKOOZ G., HOLMES P., LUMLEY J.L., 1993, The proper orthogonal decomposition in the analysis of turbulent flows, *Annu. Rev. Fluid Mech.*, **25**, 539-571

6. CITRINITI J., GEORGE W., 2000, Reconstruction of the global velocity field in the axisymmetric mixing layer utilizing the proper orthogonal decomposition, *J. Fluid Mech.*, **418**, 137-166

7. DEVILLE J., BONNET J.P., 2002, Two-point correlation in fluid dynamics: POD, LSE and related methods, In: Lecture Series on *Post-processing of experimental and numerical data*, von Karman Institute for Fluid Dynamics, Rhode-Saint-Genèse, Belgium

8. DEVILLE J., LAMBALLAIS E., BONNET J.P., 2000, POD, LODS and LSE: their links to control and simulations of mixing layers, *ERCOFTAC Bulletin*, **46**, 29-44

9. Gunes H., Rist U., 2004, Proper orthogonal decomposition reconstruction of a transitional boundary layer with and without control, *Phys. Fluids*, **16**, 2763-2784

10. Holmes P., Lumley J.L., Berkooz G., 1996, *Turbulence, Coherent Structures, Dynamical Systems and Symmetry*, Cambridge University Press

11. Iwamoto K., 2002, Database of Fully Developed Channel Flow, THTLAB Internal Report, No. ILR-0201, Dept. of Mech. Eng., The University of Tokyo

12. Joia I.A., Gobeau N., Ushijima T., Perkins R.J., 1998, POD study of bubble and particle motion in turbulent channel flow, *International Conference on Multiphase Flow*, June 8-12, Lyon, France

13. Kasagi N., Kuroda A., Hirata M., 1989, Numerical investigations of near-wall turbulent heat transfer taking into account the unsteady heat conduction in the solid wall, *J. Heat Transfer*, **111**, 385-392

14. Łuniewski M., J. Pozorski, T. Wacławczyk, 2006, LES of turbulent channel flow with dispersed particles [in Polish], *Systems*, **11**, 224-232

15. Moin P., Moser R.D., 1989, Characteristic-eddy decomposition of turbulence in a channel, *J. Fluid Mech.*, **200**, 471-508

16. Omurtag A., Sirovich L., 1999, On low-dimensional modelling of channel turbulence, *Theoret. Comput. Fluid Dynamics*, **13**, 115-127

17. Peyret R., 2002, *Spectral Methods for Incompressible Viscous Flow*, Springer-Verlag, New York

18. Picciotto M., Marchioli C., Soldati A., 2005, Characterization of near-wall accumulation regions for inertial particles in turbulent boundary layers, *Phys. Fluids*, **17**, 098101

19. Podvin B., 2001, On the adequacy of the ten-dimensional model for the wall layer, *Phys. Fluids*, **13**, 210-224

20. Pope S.B., 2000, *Turbulent Flows*, Cambridge University Press

21. Sanghi S., Aubry N., 1993, Mode interaction models for near-wall turbulence, *J. Fluid Mech.*, **244**, 455-488

22. Wacławczyk M., Pozorski J., 2002, Two-point velocity statistics and the POD analysis of the near-wall region in a turbulent channel flow, *J. Theor. Appl. Mech.*, **40**, 895-916

23. Wacławczyk M., Pozorski J., 2004, Conjugate heat transfer modelling using the FDF approach for near-wall scalar transport coupled with the POD method for flow dynamics, In: *Advances in Turbulence X*, H.I. Andersson and P.-A. Krogstad (Edit.), CIMNE, Barcelona

24. Webber G., Handler R., Sirovich L., 1997, The Karhunen-Loéve decomposition of minimal channel flow, *Phys. Fluids*, **9**, 1054-1066

Modelowanie turbulencji za pomocą wielkoskalowych modów prędkości

Streszczenie

Przedmiotem pracy jest modelowanie turbulentnego pola prędkości w obszarze przyściennym za pomocą niskowymiarowego systemu dynamicznego, opartego o dekompozycję w bazie funkcji własnych POD (ang. *Proper Orthogonal Decomposition*). Empiryczna baza funkcyjna POD została wyznaczona z rozwiązania zagadnienia własnego, w którym obecne są dwupunktowe korelacje prędkości. Następnie, w wyniku projekcji Galerkina równań pędu na podprzestrzeń rozpiętą na tej bazie funkcyjnej, otrzymano układ równań różniczkowych zwyczajnych na zależne od czasu współczynniki. Na podstawie funkcji własnych oraz z wyznaczonych współczynników rozkładu uzyskano ewolucję w czasie charakterystycznych struktur wirowych w obszarze przyściennym. System dynamiczny rozpatrywany w pracy składa się z 20 równań różniczkowych zwyczajnych. Zrekonstruowane pole prędkości jest dwuwymiarowe (w płaszczyźnie prostopadłej do głównego kierunku przepływu). Ponadto w pracy dyskutowana jest procedura filtrowania związana z metodą POD. Wyprowadzony filtr POD porównano z formułą używaną w metodzie symulacji dużych wirów.